COMPDYN 2015
5th ECCOMAS Thematic Conference on
Computational Methods in Structural Dynamics and Earthquake Engineering
M. Papadrakakis, V. Papadopoulos, V. Plevris (eds.)
Crete Island, Greece, 25–27 May 2015

MODELLING OF THE VIBRO-ACOUSTIC TRANSMISSION ON MULTI-PLATE PERFORATED PANELS USING TWO-SCALE HOMOGENIZATION

Eduard Rohan[1] **and Vladimír Lukeš**[2]

[1]Department of Mechanics, Faculty of Applied Sciences,
University of West Bohemia,
Univerzitní 22, 30614 Plzeň, Czech Republic
e-mail: rohan@kme.zcu.cz

[2]European Centre of Excellence, NTIS New Technologies for Information Society, Faculty of Applied Sciences,
University of West Bohemia,
Univerzitní 22, 30614 Plzeň, Czech Republic
e-mail: vlukes@kme.zcu.cz

Keywords: Acoustic Transmission, Multi-plate Panel, Reissner-Mindlin Plate, Homogenization

Abstract. *We consider problems of the acoustic wave propagation through panels consisting of several vibrating periodically perforated Reissner-Mindlin plates. The proposed model of the wave transmission through a layer involving the acoustic fluid and the panel is derived using the homogenization method. This provides homogenized transmission conditions which are prescribed on a flat interface representing the panel, so that the computational complexity of the vibroacoustic problem is reduced, although the geometrical arrangement of pores in the panel is respected in a detail. For a suitable mutual arrangement of holes in two, or more parallel plates there is a coupling between transverse and surface acoustic waves propagating along the panel.*

1 INTRODUCTION

The paper deals with modelling the acoustic wave propagation through vibrating perforated panels composed of several plates. Usually the models of acoustic impedance are based on semi-empirical formulae which are tuned by experiments, see e.g. [11]. Therefore, it is desirable to develop a computationally tractable model which takes into account the perforation geometry in a rigorous way. In this work we present a reduced model of the vibroacoustic transmission which is based on the two-scale homogenization [2]. For this we extend the approach developed in [6], where homogenization of rigid plates was pursued to derive effective nonlocal transmission conditions. A model of the single-plate perforated compliant panel was considered in [10] in the context the optimal perforation design problem. Using a slightly different modelling ansatz related to the plate thickness scaling, we derive a homogenized model of the acoustic transmission through a layer in which two periodically perforated elastic plates of the Reissner-Mindlin type are situated. This construction of the panel with different perforations of the two plates admits special acoustic transmission effects due to coupling the transverse and surface acoustic waves propagating along the panel.

The paper is organized, as follows. In Section 1.1 the global problem is defined which governs the wave propagation in the fluid part and in the solid part. The final form of the reduced global problem is announced in Section 1.2. In Section 2 we introduce the transmission layer containing the perforated plates and define the problem which is subject of the asymptotic analysis with respect to the layer thickness and size of the perforation. The homogenized transmission conditions are reported in Section 3. In Section 4 we illustrate the influence of some geometrical parameters of the coefficients involved in the transmission conditions.

1.1 The global problem – acoustics in perforated domain

We consider open bounded domain Ω^G which contains the compliant periodically perforated panel represented by domain Σ_ε. By ε we denote a small parameter which corresponds to the thickness of the panel and to the characteristic period of the perforation. Therefore, the labelling by superscript $^\varepsilon$ is used to indicate the dependence on size of the perforations. The problem of the acoustic harmonic wave propagation is imposed in domain Ω^G involving the solid part Σ_ε and the acoustic fluid occupying domain $\Omega^{*\varepsilon} = \Omega^G \setminus \Sigma_\varepsilon$, whereby the vibro-acoustic transmission is prescribed on interface $\Gamma^\varepsilon = \partial\Sigma_\varepsilon \cap \partial\Omega^{*\varepsilon}$. The acoustic potential p^ε and the displacement field $\boldsymbol{u}^\varepsilon$ satisfy

$$
\begin{aligned}
c^2\nabla^2 p^\varepsilon + \omega^2 p^\varepsilon = 0 \quad & \text{in } \Omega^{*\varepsilon} \;, \\
\nabla\cdot\boldsymbol{\sigma}^\varepsilon(\boldsymbol{u}^\varepsilon) = 0 \quad & \text{in } \Sigma^\varepsilon \;, \\
\left.\begin{aligned}
\boldsymbol{n}\cdot\boldsymbol{\sigma}^\varepsilon(\boldsymbol{u}^\varepsilon) & = \mathrm{i}\omega\rho_0 p^\varepsilon \boldsymbol{n} \;, \\
\boldsymbol{n}\cdot\nabla p^\varepsilon & = -\mathrm{i}\omega \boldsymbol{n}\cdot\boldsymbol{u}^\varepsilon \;,
\end{aligned}\right\} \quad & \text{on } \Gamma^\varepsilon \;, \\
\boldsymbol{u} = 0 \quad & \text{on } \partial\Sigma^\varepsilon \setminus \Gamma^\varepsilon \;, \\
\text{boundary conditions} \quad & \text{on } \partial\Omega^G \;,
\end{aligned}
\tag{1}
$$

where ω is the wave frequency, c is the speed of sound propagation, $\boldsymbol{\sigma}(\boldsymbol{u}) = \mathbb{D}\nabla^S\boldsymbol{u}$ is the stress tensor related to the strain $\nabla^S\boldsymbol{u}$ by the (3D) elasticity tensor $\mathbb{D}$, and $\boldsymbol{n}$ is the normal vector.

The solid elastic body Σ^ε is constituted by elastic plates Σ_K^ε, thus $\Sigma^\varepsilon = \bigcup_K \Sigma_K^\varepsilon$. Behaviour of each elastic plate Σ_K^ε is described using the Reissner-Mindlin (R-M) plate model whereby the generalized loads are derived by taking into account the specific perforation geometry and the loading by the acoustic field; to derive them, the R-M plate kinematic constraints of deformation are considered.

For each plate $K = I, II$ represented by the perforated mid-plane, i.e. by the domain $\Gamma_K^\varepsilon \subset \Gamma_K$, specified by its thickness $h_K^\varepsilon = \varepsilon \bar{h}_K$, and by the elastic coefficients $\mathbb{C}, \gamma$, the following equations in Γ_K^ε govern the plate displacements $(\boldsymbol{u}^{\varepsilon,K}, w^{\varepsilon,K})$ and rotations $\boldsymbol{\theta}^{\varepsilon,K}$ (below in equation (2) the suffix K is omitted for brevity)

$$\left\{ \begin{array}{rcl} -\omega^2 h^\varepsilon \rho \boldsymbol{u}^\varepsilon - h^\varepsilon \overline{\nabla} \cdot [\mathbb{C} \overline{\nabla}^S (\boldsymbol{u}^\varepsilon)] & = & \boldsymbol{t}^\varepsilon \ , \\ -\omega^2 h^\varepsilon \rho w^\varepsilon - h^\varepsilon \overline{\nabla} \cdot [\gamma(\overline{\nabla} w^\varepsilon - \boldsymbol{\theta}^\varepsilon)] & = & f^\varepsilon \ , \\ -\omega^2 \frac{(h^\varepsilon)^3}{12} \rho \boldsymbol{\theta}^\varepsilon - \frac{(h^\varepsilon)^3}{12} \mathrm{div}[\mathbb{C} \overline{\nabla}^S (\boldsymbol{\theta}^\varepsilon)] & & \\ -h^\varepsilon \gamma (\overline{\nabla} w^\varepsilon - \boldsymbol{\theta}^\varepsilon) & = & \overline{\boldsymbol{m}}^\varepsilon \ , \end{array} \right. \tag{2}$$

where $\overline{\nabla} = (\partial_\alpha)$, $\alpha = 1, 2$ is the "in-plane" gradient, $\boldsymbol{t}^\varepsilon = (\bar{b}_\alpha)$, $f^\varepsilon = \bar{b}_3$ are derived from the boundary traction forces $\boldsymbol{b}^\varepsilon = \mathrm{i}\omega\rho_0 \boldsymbol{n} p^\varepsilon$ acting on the 3D representation of the plate and involving the acoustic potential p^ε. The plates are clamped on $\partial\Gamma_K$ and the Neumann conditions corresponding to the traction forces being expressed in terms of p^ε, are prescribed on the holes $\partial\Gamma_K^\varepsilon \setminus \partial\Gamma_K$.

1.2 Limit global problem

The aim of the work reported in this paper was to derive a limit problem describing the wave propagation in a homogenized layer containing the panel, so that transmission conditions can be obtained which allow for reformulation of problem (1) in domain $\Omega^G = \Omega^+ \cup \Omega^- \cup \Gamma_0$, where Ω^+ and Ω^- are non-overlapping parts and the planar surface Γ_0 represents the panel. The main result is formulation of the following "reduced" problem of the vibro-acoustic wave propagation: Find p such that

$$\begin{aligned} c^2 \nabla^2 p + \omega^2 p = 0 \quad & \text{in } \Omega^+ \cup \Omega^- \ , \\ \frac{\partial p}{\partial n} = \pm \mathrm{i}\omega g^0 \quad & \text{on } \Gamma^\pm \ , \\ \text{boundary conditions} \quad & \text{on } \partial\Omega^G \ , \\ \mathcal{G}([p]_-^+, g^0) = 0 \quad & \text{on } \Gamma_0 \end{aligned} \tag{3}$$

where $\Gamma^\pm = \partial\Omega^\pm \cap \Gamma_0$, $[p]_-^+ = p|_{\Gamma^+} - p|_{\Gamma^-}$ and $\mathcal{G}(\cdot,\cdot)$ is an implicit form of the transmission conditions on interface Γ_0 which describe the behaviour of the perforated multi-plate panel; it is constituted by the homogenized model given in Section 3.3, equations (42). In fact, $\mathcal{G}$ represents the Dirichlet-to-Neumann operator.

2 Problem in the transmission layer

In this section we describe the model of the vibroacoustic transmission which was subject of the homogenization procedure leading to the limit problem reported in Section 3. By $\Gamma_0 \subset \mathbb{R}^2$ we designate the mid-plane of the layer $\Omega_\delta \subset \mathbb{R}^3$ bounded by surfaces Γ_δ^+ and Γ_δ^- equidistant to Γ_0 with the distance $\delta/2$, so that $\Omega_\delta = \Gamma_0 \times] - \delta/2, \delta/2[\subset \mathbb{R}^3$. Recall that ε is the characteristic size of the perforation of all the plates, whereby $\delta = \varkappa\varepsilon$ for a given $\varkappa > 0$, see Fig. 1.

The microstructure of the perforation is periodic, being generated by the representative periodic cell $Y = \Xi \times \varkappa] - 1/2, +1/2]$, where $\Xi =]0, b_1[\times]0, b_2[$. Further we define the solid part $S \subset Y$ such that

$$S = \bigcup_K \Xi_K^S \times \left(\bar{h}] - 1/2, +1/2] + \hat{z}_K \right) \ , \tag{4}$$

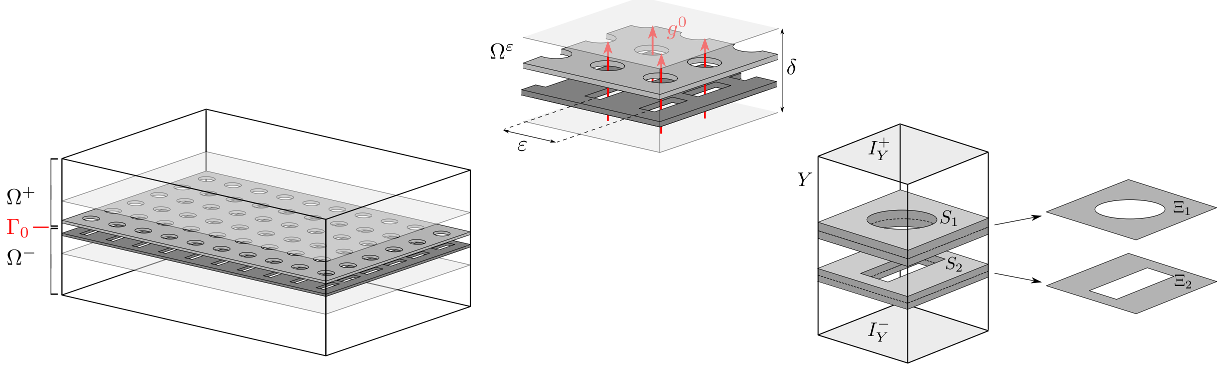

Figure 1: Scheme of the transmission layer with 2 plates. The layer thickness $\delta = \varkappa\varepsilon$, the plate thickness $h_K^\varepsilon = \varepsilon\bar{h}_K$

where $\Xi_K^S \subset \Xi$ represents the K-th plate perforated mid-plane and $\hat{z}_K$ is the "vertical" dilated position of the plate mid-plane. Using $Y^* = Y \setminus \overline{S}$ we define

$$\Omega^\varepsilon = \bigcup_{k\in\mathbb{Z}^2} \varepsilon(Y^* + \sum_{i=1,2} k_i b_i \vec{e_i}) \cap \Omega_\delta \,, \tag{5}$$

where $\Omega^\varepsilon = \Omega_\delta \setminus \Sigma^\varepsilon$ is the domain occupied by the fluid. We introduce the solid part of the layer $\Sigma^\varepsilon = \Omega_\delta \setminus \Omega^\varepsilon$. By $\hat{x}_3^K$ we denote the (non-dilated) transverse position of the K-th plate mid-plane, $\bar{x}_3^{\pm K}$ is the (non-dilated) transverse position of the K-th plate upper(+) and lower(-) surfaces.The solid panel is formed by individual plates Σ_K^ε, so that

$$\begin{aligned} \Sigma^\varepsilon &= \bigcup_{K=I,II} \Sigma_K^\varepsilon \,, \quad \Sigma_K^\varepsilon = \Gamma_K^\varepsilon \times h_K^\varepsilon]-1/2, 1/2[\,, \\ \Gamma_K^\varepsilon &= \bigcup_{k\in\mathbb{Z}^2} \left(\hat{x}_3^K + \varepsilon \left(\Xi_K + \sum_{i=1,2} k_i b_i \vec{e_i} \right) \cap \Gamma_0 \right) \,. \end{aligned} \tag{6}$$

Thus, Γ_K^ε is the "2D" representation of the K-th plate which has its thickness $h_K^\varepsilon = \varepsilon\bar{h}_K$.

Through the paper we use the following decomposition of coordinates: for $x \in \Omega^G$, the position can be written as $x = (x', x_3)$ where $x' \in \Gamma_0$; for $y \in Y$, we have $y = (y', z)$ where $y' \in \Xi$.

2.1 Acoustic problem in the layer

To derive the acoustic transmission conditions, we consider the vibro-acoustic problem in the layer. The total acoustic potential, p^ε satisfies the Helmholtz equation in Ω^ε and Neumann conditions on $\partial\Omega^\varepsilon$

$$\begin{aligned} & c^2\nabla^2 p^\varepsilon + \omega^2 p^\varepsilon = 0 \quad \text{in } \Omega^{\varepsilon\delta} \,, \\ \text{velocity of "external" fluid} \quad & \frac{\partial p^\varepsilon}{\partial n} = -\mathrm{i}\omega g^{\varepsilon\pm} \quad \text{on } \Gamma^{\pm\delta} \,, \\ \text{velocity of solid structure} \quad & \frac{\partial p^\varepsilon}{\partial n} = -\mathrm{i}\omega \boldsymbol{n}\cdot\boldsymbol{u}^\varepsilon \quad \text{on } \partial\Sigma^\varepsilon \,, \\ & \frac{\partial p^\varepsilon}{\partial n} = 0 \quad \text{on } \partial\Omega^{\delta\infty} \,, \end{aligned} \tag{7}$$

where $g^{\varepsilon\pm}$ is the given data representing the transverse acoustic velocity which couples the problem (7) with the global problem (3). The surface $\partial\Omega^\varepsilon$ splits into disjoint parts, $\partial\Omega^\varepsilon =$

$\partial\Sigma^\varepsilon \cup \Gamma_\delta^+ \cup \Gamma_\delta^- \cup \partial\Omega^{\delta\infty}$, where $\partial\Omega^{\delta\infty}$ represents the fixed wall of a duct in which the panel is fitted.

The response of the solid panel is governed by the plate equations (2) adapted for each plate (note that this set of equations describes one plate) where the r.h.s. terms are expressed in terms of the acoustic potential p^ε.

2.2 Weak formulation of the coupled vibroacoustic problem

We write the system of equations describing the fluid and the structure response to the transverse acoustic velocity $\mathrm{i}\omega g^{\varepsilon\pm}$. It consists of three parts:

1. Acoustic fluid response p^ε in the transmission layer responds to the excitation by the transverse acoustic velocity $\mathrm{i}\omega g^{\varepsilon\pm}$ on the upper and lower boundary and by the vibrating structure. In the dilated configuration, where the layer has the thickness $\varkappa$, the acoustic potential $p^\varepsilon(x', z)$ satisfies

$$\begin{aligned} c^2 \int_{\Omega^\varepsilon} \hat{\nabla} p^\varepsilon \cdot \hat{\nabla} q^\varepsilon - \omega^2 \int_{\Omega^\varepsilon} p^\varepsilon q^\varepsilon = -\frac{\mathrm{i}\omega c^2}{\varepsilon} \int_{\Gamma^\pm} \hat{g}^{\varepsilon\pm} q^\varepsilon - \frac{\mathrm{i}\omega c^2}{\varepsilon} \sum_{K=I,II} \int_{\Gamma_K^\varepsilon} w^{\varepsilon,K} \langle q^\varepsilon \rangle_{K-}^{K+} \\ -\frac{\mathrm{i}\omega c^2}{\varepsilon} \sum_{K=I,II} \int_{\partial\Gamma_K^\varepsilon} \varepsilon \bar{h}_K \int_{-1/2}^{1/2} \bar{\boldsymbol{n}} \cdot (\boldsymbol{u}^{\varepsilon,K} - \varepsilon \bar{h}_K \zeta \boldsymbol{\theta}^{\varepsilon,K}) q^\varepsilon(\cdot, \hat{x}_3^K + \varepsilon \bar{h}_K \zeta) \mathrm{d}\zeta \;, \end{aligned} \tag{8}$$

   for all q^ε where $\hat{\nabla} = (\overline{\nabla}, \frac{1}{\varepsilon}\partial_z)$, recalling $\overline{\nabla} = (\partial_\alpha)$, $\alpha = 1, 2$ is the "in-plane" gradient, $\bar{\boldsymbol{n}} = (n_\alpha)$ is the in-plane normal vector, and $\langle p^1 \rangle_{K-}^{K+} = v(\cdot, \bar{x}_3^{+K}) - v(\cdot, \bar{x}_3^{-K})$.

2. For each plate K, the deflection – rotation modes $(w^{\varepsilon,K}, \boldsymbol{\theta}^{\varepsilon,K})$ response to the loading by the acoustic pressure p^ε is governed by the following equation, where $(v_3^\varepsilon, \boldsymbol{\vartheta}^\varepsilon)$ are test functions:

$$\begin{aligned} -\omega^2 \int_{\Gamma_K^\varepsilon} \rho_S \left[\varepsilon \bar{h}_K w^\varepsilon v_3^\varepsilon + \varepsilon^3 \frac{\bar{h}_K^3}{12} \boldsymbol{\theta}^\varepsilon \cdot \boldsymbol{\vartheta}^\varepsilon \right] \\ +\varepsilon^3 \frac{\bar{h}_K^3}{12} \int_{\Gamma_K^\varepsilon} \mathbb{C}_K^\varepsilon \overline{\nabla}^S \boldsymbol{\theta}^\varepsilon : \overline{\nabla}^S \boldsymbol{\vartheta}^\varepsilon + \varepsilon \bar{h}_K \int_{\Gamma_K^\varepsilon} \gamma_K (\overline{\nabla} w^\varepsilon - \boldsymbol{\theta}^\varepsilon) \cdot (\overline{\nabla} v_3^\varepsilon - \boldsymbol{\vartheta}^\varepsilon) \\ = \mathrm{i}\omega\rho_0 \left[\int_{\Gamma_K^\varepsilon} v_3^\varepsilon \langle p^\varepsilon \rangle_{K-}^{K+} + (\varepsilon \bar{h}_K)^2 \int_{\partial\Gamma_K^\varepsilon} \int_{-1/2}^{1/2} p^\varepsilon(\cdot, \hat{x}_3^K + \varepsilon \bar{h}_K \zeta) \bar{\boldsymbol{n}} \cdot (-\zeta \boldsymbol{\vartheta}^\varepsilon) \mathrm{d}\zeta \right] \;, \end{aligned} \tag{9}$$

   where $\overline{\nabla}^S = \frac{1}{2}(\overline{\nabla}^T + \overline{\nabla})$.

3. For each plate K, the in-plane deformation described by displacements $\boldsymbol{u}^{\varepsilon,K}$ is the response to the loading by the acoustic pressure p^ε, where $\boldsymbol{v}^\varepsilon$ is the test function:

$$\begin{aligned} -\omega^2 \varepsilon \bar{h}_K \int_{\Gamma_K^\varepsilon} \rho_S \boldsymbol{u}^\varepsilon \cdot \boldsymbol{v}^\varepsilon + \varepsilon \bar{h}_K \int_{\Gamma_K^\varepsilon} \mathbb{C}_K^\varepsilon \overline{\nabla}^S \boldsymbol{u}^\varepsilon : \overline{\nabla}^S \boldsymbol{v}^\varepsilon \\ = \mathrm{i}\omega\rho_0 \varepsilon \bar{h}_K \int_{\partial\Gamma_K^\varepsilon} \bar{\boldsymbol{n}} \cdot \boldsymbol{v}^\varepsilon \int_{-1/2}^{1/2} p^\varepsilon(\cdot, \hat{x}_3^K + \varepsilon \bar{h}_K \zeta) \mathrm{d}\zeta \end{aligned} \tag{10}$$

Weak formulation. For given external transverse velocities $g^{\varepsilon\pm}$ defined on $\Gamma^\pm$, find $(\boldsymbol{u}^{\varepsilon,K}, w^{\varepsilon,K}, \boldsymbol{\theta}^{\varepsilon,K})$ for $K = I, II$ and p^ε such that equations (9),(10) and (8) hold for all test functions $(q^\varepsilon, \boldsymbol{v}^\varepsilon, v_3^\varepsilon, \boldsymbol{\vartheta}^\varepsilon)$.

2.3 Coupling of the layer with external acoustic fields

The following coupling identity is considered, which expresses the jump of the exterior field $p_{\rm ext}$ across the layer with finite $\delta > 0$,

$$\int_{\Gamma_\delta^+} p_{\rm ext}^{\delta+} - \int_{\Gamma_\delta^-} p_{\rm ext}^{\delta-} = \int_{\Gamma_0} \int_{-\delta/2}^{\delta/2} \partial_{x_3} \tilde{p}^\varepsilon \quad \forall \psi \in L^2(\Gamma_0)\;, \tag{11}$$

where we assume $\psi = \psi(x')$, $x' \in \Gamma_0$, and by $\tilde{}$ we denote an extension of p^ε to the whole Ω_δ. We may apply the dilation formula at the r.h.s. of (11) to get

$$\left(\int_{\Gamma_\delta^+} p_{\rm ext}^{\delta+} - \int_{\Gamma_\delta^-} p_{\rm ext}^{\delta-}\right) \approx \int_{\Gamma_0} (p_{\rm ext}^{\delta_0+} - p_{\rm ext}^{\delta_0-}) = \varepsilon \int_{\Gamma_0} \int_{-\varkappa/2}^{\varkappa/2} \frac{1}{\varepsilon} \partial_z \tilde{p}^\varepsilon \quad \forall \psi \in L^2(\Gamma_0)\;. \tag{12}$$

Further we consider a finite layer thickness $\delta_0 = \varkappa \varepsilon_0 > 0$ in the l.h.s. expression of (12), whereas we pass to the limit on its r.h.s. , so that we obtain the following approximation of the discontinuity of $p_{\rm ext}$ along Γ_0:

$$\begin{aligned} \frac{1}{\varepsilon_0} \int_{\Gamma_0} (p_{\rm ext}^{\delta_0+} - p_{\rm ext}^{\delta_0-}) &\approx \lim_{\varepsilon \to 0} \int_{\Gamma_0} \int_{-\varkappa/2}^{\varkappa/2} \frac{1}{\varepsilon} \fint_{\Xi} \partial_z \mathcal{T}_\varepsilon(\tilde{p}^\varepsilon) \\ &= \int_{\Gamma_0} \int_{-\varkappa/2}^{\varkappa/2} \fint_{\Xi} \partial_z \tilde{p}^1 = \int_{\Gamma_0} \psi [\tilde{p}^1]_-^+ \\ &= \int_{\Gamma_0} \left(\fint_{I_y^+} p^1 - \fint_{I_y^-} p^1 \right) \quad \forall \psi \in L^2(\Gamma_0)\;. \end{aligned} \tag{13}$$

3 Homogenized transmission layer

The asymptotic analysis of problem (9),(10), and (8) yields the recovery sequences $\boldsymbol{Q}^{R\varepsilon} = (p^{0,\varepsilon}, p^{1,\varepsilon}, \boldsymbol{u}^{0,K\varepsilon}, \boldsymbol{u}^{1,K\varepsilon}, w^{0,K\varepsilon}, w^{1,K\varepsilon}, \boldsymbol{\theta}^{K\varepsilon})$ which allow us to obtain the limit homogenized two-scale model of the wave propagation in the transmission layer; the following truncated expansions hold, where $x' \in \Gamma^0$ and

$$\begin{aligned} p^\varepsilon(x) &\approx p^{0,\varepsilon}(x') + \varepsilon p^{1,\varepsilon}(x', y', z)\;, \quad y' \in \Xi\;, \quad z \in [-1/2, +1/2]\;, \\ \boldsymbol{u}^{K,\varepsilon}(x') &\approx \boldsymbol{u}^{0,K\varepsilon}(x') + \varepsilon \boldsymbol{u}^{1,K\varepsilon}(x', y')\;, \quad y' \in \Xi_K\;, \\ w^{K,\varepsilon}(x') &\approx w^{0,K\varepsilon}(x') + \varepsilon w^{1,K\varepsilon}(x', y')\;, \quad y' \in \Xi_K\;, \\ \boldsymbol{\theta}^\varepsilon(x') &\approx \boldsymbol{\theta}^{K\varepsilon}(x', y')\;, \quad y' \in \Xi_K\;, \end{aligned} \tag{14}$$

where $x' \in \Gamma^0$. The functions $\boldsymbol{Q}^{R\varepsilon}$ converge in the unfolded space to the limit functions $\boldsymbol{Q}$, where $\boldsymbol{Q} = (p^0, p^1, \boldsymbol{u}^{0,K}, \boldsymbol{u}^{1,K}, w^{0,K}, w^{1,K}, \boldsymbol{\theta}^K)$ which are the solutions of the homogenized problem arising from (8),(9), and (10) for $\varepsilon \to 0$. Note that all functions in $\boldsymbol{Q}$ are Ξ-periodic in the y' variable; we use the space $H^1_{\#}(Y) \subset H^1(Y)$ containing only Ξ-periodic functions.

3.1 Local problems and scale decoupling

From the limit of equation (8), the following identity can be obtained which holds for a.a. $x' \in \Gamma_0$,

$$
\begin{aligned}
&\fint_{Y^*} (\overline{\nabla}_x p^0 + \overline{\nabla}_y p^1) \cdot \overline{\nabla}_y q^1 + \fint_{Y^*} \partial_z p^1 \partial_z q^1 = -\mathrm{i}\omega g^0 \left(\fint_{I_y^+} q^1 - \fint_{I_y^-} q^1 \right) \\
&- \mathrm{i}\omega \left[\sum_{K=I,II} \left(w^{0,K} \fint_{\Xi_K} \langle q^1 \rangle_{K-}^{K+} + \bar{h}_K \boldsymbol{u}^0 \cdot \fint_{\Gamma_{\Xi}^K} \bar{\boldsymbol{n}} \int_{-1/2}^{1/2} q^1(x', y', \hat{z}_K + \bar{h}_K \zeta) \mathrm{d}\zeta \right) \right] ,
\end{aligned} \tag{15}
$$

for all $q^1 \in H^1_{\underline{\#}}(Y^*)$. Due to linearity, the following split can be introduced:

$$
p^1 = \pi^\beta \partial_\beta^x p^0 + \mathrm{i}\omega \left[\xi g^0 + \sum_{K=I,II} \left(\eta_K w^{0,K} + \mu_K^\alpha u_\alpha^{0,K} \right) \right] , \tag{16}
$$

where the corrector basis functions $\pi^\beta, \xi, \eta_K, \mu_K^\alpha$ which are Ξ-periodic are solutions of the local problems: Find $\pi^\beta, \xi, \eta_K, \mu_K^\alpha \in H^1_{\underline{\#}}(Y^*)/\mathbb{R}$ such that

$$
\begin{aligned}
&\fint_{Y^*} \nabla_y \pi^\beta \cdot \nabla_y \psi = -\fint_{Y^*} \partial_\beta^y \psi , \\
&\fint_{Y^*} \nabla_y \xi \cdot \nabla_y \psi = -\left(\fint_{I_y^+} \psi - \fint_{I_y^-} \right) , \\
&\fint_{Y^*} \nabla_y \eta_K \cdot \nabla_y \psi = -\fint_{\Xi_K} \left(\psi(\cdot, \bar{z}^{K+}) - \psi(\cdot, \bar{z}^{K-}) \right) = -\fint_{\Xi_K} \langle \psi \rangle_{K-}^{K+} , \\
&\fint_{Y^*} \nabla_y \mu_K^\beta \cdot \nabla_y \psi = -\bar{h}_K \fint_{\Gamma_{\Xi}^K} n_\beta \int_{-1/2}^{1/2} \psi(\cdot, \hat{z}^K + \zeta) \mathrm{d}\zeta ,
\end{aligned} \tag{17}
$$

for all $\psi \in H^1_{\underline{\#}}(Y^*)$, where $\bar{z}^{K\pm} = \hat{z}^K \pm \frac{\bar{h}_K}{2}$ and recalling $\nabla_y = (\partial_\alpha^y, \partial_z)$.

Next we consider the limit form of the plate deflection-rotation arising from (9); for a.a. $x' \in \Gamma_0$, we obtain

$$
\frac{\bar{h}_K^3}{12} \fint_{\Xi_K} \mathbb{C} \overline{\nabla}_y^S \boldsymbol{\theta} : \overline{\nabla}_y^S \boldsymbol{\vartheta} + \bar{h}_K \int_{\Xi_K} \gamma \big(\overline{\nabla}_x w^0 + \overline{\nabla}_y w^1 - \boldsymbol{\theta} \big) \cdot \big(\overline{\nabla}_y v^1 - \boldsymbol{\vartheta} \big) = 0 , \tag{18}
$$

for all $v^1 \in H^1_\#(\Xi_K), \boldsymbol{\vartheta} \in [H^1_\#(\Xi_K)]^2$. Using the corrector basis functions $\chi_K^\alpha \in H^1_\#(\Xi_K)/\mathbb{R}$ and $\boldsymbol{\varphi}_K^\alpha \in [H^1_\#(\Xi_K)]^2$ we introduce the split

$$
w^{1,K} = \chi_K^\alpha \partial_\alpha^x w^{0,K} , \quad \boldsymbol{\theta}^K = \boldsymbol{\varphi}_K^\alpha \partial_\alpha^x w^{0,K} , \tag{19}
$$

where the couple $(\boldsymbol{\varphi}_K^\alpha, \chi_K^\alpha)$ satisfies

$$
\begin{aligned}
\frac{\bar{h}_K^2}{12} \fint_{\Xi_K} \mathbb{C} \overline{\nabla}_y^S \boldsymbol{\varphi}_K^\alpha : \overline{\nabla}_y^S \boldsymbol{\psi} + \fint_{\Xi_K} \gamma (\overline{\nabla}_y \chi_K^\alpha - \boldsymbol{\varphi}_K^\alpha) \cdot (\overline{\nabla}_y v - \boldsymbol{\psi}) = -\fint_{\Xi_K} \gamma (\partial_\alpha^y v - \psi_\alpha) \\
\forall v \in H^1_\#(\Xi_K), \ \boldsymbol{\psi} \in [H^1_\#(\Xi_K)]^2 .
\end{aligned} \tag{20}
$$

Finally we consider the limit of (10) describing the "in-plane" deformation of the plate. This yields, for a.a. $x' \in \Gamma_0$,

$$\bar{h}_K \fint_{\Xi_K} \mathbb{C}(\overline{\nabla}_x^S \boldsymbol{u}^{0,K} + \overline{\nabla}_y^S \boldsymbol{u}^{1,K}) : \overline{\nabla}_y^S \boldsymbol{v}^1 = \mathrm{i}\omega\rho_0 \bar{h}_K p^0 \fint_{\Gamma_\Xi^K} \boldsymbol{n} \cdot \boldsymbol{v}^1 \;, \tag{21}$$

for all $\boldsymbol{v}^1 \in [H^1_\#(\Xi_K)]^2$. Using the corrector basis functions $\boldsymbol{\chi}_K^{\alpha\beta}, \boldsymbol{\chi}_K^P \in [H^1_\#(\Xi_K)]^2$ we define the split

$$\boldsymbol{u}^{1,K} = \boldsymbol{\chi}_K^{\alpha\beta} \partial_\beta u_\alpha^{0,K} + \mathrm{i}\omega\rho_0 \boldsymbol{\chi}_K^P p^0 \;, \tag{22}$$

where the following two local corrector problem must be solved:

$$\begin{aligned} \fint_{\Xi_K} \mathbb{C}\overline{\nabla}_y^S (\boldsymbol{\chi}_K^{\alpha\beta} + \boldsymbol{\Pi}^{\alpha\beta}) : \overline{\nabla}_y^S \boldsymbol{v} = 0 \quad \forall \boldsymbol{v} \in [H^1_\#(\Xi_K)]^2 \;, \\ \fint_{\Xi_K} \mathbb{C}\overline{\nabla}_y^S \boldsymbol{\chi}_K^P : \overline{\nabla}_y^S \boldsymbol{v} = \fint_{\Gamma_\Xi^K} \boldsymbol{n} \cdot \boldsymbol{v} \quad \forall \boldsymbol{v} \in [H^1_\#(\Xi_K)]^2 \;. \end{aligned} \tag{23}$$

3.2 Macroscopic equations and Homogenized coefficients

In this section we introduce the homogenized coefficients involved in the limit transmission problem. From the limit form of equation (8), we obtain the following identity related to the acoustic fluid response:

$$\begin{aligned} & c^2 \int_{\Gamma_0} \fint_{Y^*} (\overline{\nabla}_x p^0 + \overline{\nabla}_y p^1) \cdot \overline{\nabla}_x q^0 - \omega^2 \int_{\Gamma_0} \fint_{Y^*} p^0 q^0 \\ & = -\mathrm{i}\omega c^2 \int_{\Gamma_0} q^0 \left[\left(\fint_{I_y^+} g^{1+} - \fint_{I_y^-} g^{1-} \right) + \bar{h}_K \sum_{K=I,II} \left(\fint_{\Gamma_\Xi^K} \bar{\boldsymbol{n}} \cdot \boldsymbol{u}^1 - \bar{h}_K \fint_{\Gamma_\Xi^K} \bar{\boldsymbol{n}} \cdot \boldsymbol{\theta}^K \int_{-1/2}^{1/2} \zeta \right) \right] \;. \end{aligned} \tag{24}$$

Using the split formulae (16), (19) and (22), the homogenized coefficients are computed:

$$\begin{aligned} A_{\alpha\beta} &= \fint_{Y^*} \nabla_y (\pi^\beta + y_\beta) \cdot (\pi^\alpha + y_\alpha) \;, \\ B_\alpha &= \fint_{Y^*} \partial_\alpha^y \xi \;, \\ P_\alpha^K &= \fint_{Y^*} \partial_\alpha^y \eta_K \;, \\ R_{\alpha\beta}^K &= \fint_{Y^*} \partial_\alpha^y \mu_K^\beta \;, \\ S_{\alpha\beta}^K &= \bar{h}_K \fint_{\Gamma_\Xi^K} \boldsymbol{n} \cdot \boldsymbol{\chi}_K^{\alpha\beta} \;, \\ T^K &= \fint_{\Gamma_\Xi^K} \boldsymbol{n} \cdot \boldsymbol{\chi}_K^P \;, \end{aligned} \tag{25}$$

Further, we substitute the split form of p^1 (16) in (13) which yields the following coefficients:

$$
\begin{aligned}
F &= -\fint_{I_y^+} \xi + \fint_{I_y^-} \xi = \fint_{Y^*} \nabla_y \xi \cdot \nabla_y \xi \;, \\
C_\alpha &= \fint_{I_y^+} \pi^\alpha - \fint_{I_y^-} \pi^\alpha = -\fint_{Y^*} \nabla_y \xi \cdot \nabla_y \pi^\alpha = B_\alpha \;, \\
W^K &= \fint_{I_y^+} \eta_K - \fint_{I_y^-} \eta_K = -\fint_{Y^*} \nabla_y \xi \cdot \nabla_y \eta_K = -N^K \;, \\
X_\alpha^K &= \fint_{I_y^+} \mu_K^\alpha - \fint_{I_y^-} \mu_K^\alpha = -\fint_{Y^*} \nabla_y \xi \cdot \nabla_y \mu_K^\alpha = -N_\alpha^K \;.
\end{aligned}
\tag{26}
$$

From (9), we obtain the following identity related to the K-th plate deflection response:

$$
-\omega^2 \bar{h}_K \int_{\Gamma_K} \Big(\fint_{\Xi_K} \rho_S\Big) w^0 v^0 + \bar{h}_K \int_{\Gamma_K} \gamma \big(\overline{\nabla}_x w^0 + \overline{\nabla}_y w^1 - \boldsymbol{\theta}\big) \cdot \overline{\nabla}_x v^0 = \mathrm{i}\omega\rho_0 \int_{\Gamma_K} v^0 \fint_{\Xi_K} \langle p^1 \rangle_{K-}^{K+} \;.
\tag{27}
$$

Using the split formulae (16), (19) and (22), the following homogenized coefficients are identified:

$$
\begin{aligned}
G_{\alpha\beta}^K &= \fint_{\Xi_K} \gamma \left[\overline{\nabla}_y (y_\alpha + \chi_K^\alpha) - \boldsymbol{\varphi}_K^\alpha\right] \cdot \overline{\nabla}_y y_\beta \\
&= \fint_{\Xi_K} \left[\gamma \delta_{\alpha\beta} - \frac{\bar{h}_K^2}{12} \mathbb{C} \overline{\nabla}_y^S \boldsymbol{\varphi}^\alpha : \overline{\nabla}_y^S \boldsymbol{\varphi}^\beta + \gamma \overline{\nabla}_y (\chi_K^\alpha - \boldsymbol{\varphi}^\alpha) \cdot (\chi_K^\beta - \boldsymbol{\varphi}^\beta)\right] \;, \\
D_\beta^K &= \fint_{\Xi_K} \langle \pi^\beta \rangle_{K-}^{K+} = P_\beta^K \;, \\
M_{33}^{KL} &= -\fint_{\Xi_K} \langle \eta_L \rangle_{K-}^{K+} \;, \\
M_{3\alpha}^{KL} &= -\fint_{\Xi_K} \langle \mu_L^\alpha \rangle_{K-}^{K+} = M_{\alpha 3}^{,LK} \;, \\
N^K &= -\fint_{\Xi_K} \langle \xi \rangle_{K-}^{K+} = \fint_{Y^*} \nabla_y \eta_K \cdot \nabla_y \xi \;.
\end{aligned}
\tag{28}
$$

In analogy, from (10), we obtain the identity related to the K-th plate in-plane deformation response:

$$
\begin{aligned}
-\omega^2 \bar{h}_K \int_{\Gamma_K} \Big(\fint_{\Xi_K} \rho_S\Big) \boldsymbol{u}^0 \cdot \boldsymbol{v}^0 + \bar{h}_K \int_{\Gamma_K} \fint_{\Xi_K} \mathbb{C} (\overline{\nabla}_x^S \boldsymbol{u}^0 + \overline{\nabla}_y^S \boldsymbol{u}^1) : \overline{\nabla}_x^S \boldsymbol{v}^0 \\
= \mathrm{i}\omega\rho_0 \bar{h}_K \int_{\Gamma_K} \boldsymbol{v}^0 \cdot \fint_{\Gamma_\Xi^K} \boldsymbol{n} \int_{-1/2}^{1/2} p^1(\cdot, \hat{z}^K + \zeta) \mathrm{d}\zeta \;.
\end{aligned}
\tag{29}
$$

Upon substituting there the split formulae (16), (19) and (22), the following homogenized coefficients and their alternative expressions are obtained, where $\boldsymbol{\Pi}^{ij} = (\Pi_k^{ij})$, with $\Pi_k^{ij} = y_j \delta_{ik}$

with $i,j,k,l = 1,2$,

$$
\begin{aligned}
C_{ijkl}^K &= \bar{h}_K \oint_{\Xi_K} \mathbb{C}\overline{\nabla}_y^S(\boldsymbol{\chi}^{kl} + \boldsymbol{\Pi}^{kl}) : \overline{\nabla}_y^S(\boldsymbol{\chi}^{ij} + \boldsymbol{\Pi}^{ij}) \;, \\
Q_{\alpha\beta}^K &= \bar{h}_K \oint_{\Xi_K} \mathbb{C}\overline{\nabla}_y^S \boldsymbol{\chi}_K^P : \overline{\nabla}_y^S \boldsymbol{\Pi}^{\alpha\beta} = -S_{\alpha\beta}^K \;, \\
Z_{\alpha\beta}^K &= \bar{h}_K \oint_{\Gamma_\Xi^K} n_\alpha \int_{-1/2}^{1/2} \pi^\beta(\cdot, \hat{z}^K + \zeta)\mathrm{d}\zeta = \oint_{Y^*} \nabla_y \mu_K^\alpha \cdot \nabla_y \pi^\beta = -R_{\beta\alpha}^K \;, \\
M_{\alpha\beta}^{KL} &= -\bar{h}_K \oint_{\Gamma_\Xi^K} n_\alpha \int_{-1/2}^{1/2} \eta_L(\cdot, \hat{z}^K + \zeta)\mathrm{d}\zeta = \oint_{Y^*} \nabla_y \mu_K^\alpha \cdot \nabla_y \mu_L^\beta \;, \\
M_{\alpha 3}^{\prime KL} &= -\bar{h}_K \oint_{\Gamma_\Xi^K} n_\alpha \int_{-1/2}^{1/2} \mu_L^\beta(\cdot, \hat{z}^K + \zeta)\mathrm{d}\zeta = \oint_{Y^*} \nabla_y \mu_K^\alpha \cdot \nabla_y \eta_L = M_{3\alpha}^{LK} \;, \\
N_\alpha^K &= -\bar{h}_K \oint_{\Gamma_\Xi^K} n_\alpha \int_{-1/2}^{1/2} \xi(\cdot, \hat{z}^K + \zeta)\mathrm{d}\zeta = \oint_{Y^*} \nabla_y \mu_K^\alpha \cdot \nabla_y \xi \;.
\end{aligned}
\tag{30}
$$

3.3 Homogenized vibroacoustic problem

Using the homogenized coefficients defined above, the macroscopic model of the vibroacoustic response in the layer can be derived from equations (24), (27), (29), and (13). For brevity, we present the problem defined on Γ_0 using differential equations (31)-(34), whereby the clamped plate boundary conditions and the rigid wall condition for p^0 at $\partial\Gamma_0$ are considered.

$$
\begin{aligned}
-\omega^2 &\left[\frac{\overline{\rho_S}^K}{\rho_0} \bar{h}_K \boldsymbol{u}^{0,K} + \sum_{L=I,II} \left(M_{\alpha\beta}^{KL} u_\beta^{0,L} + M_{\alpha 3}^{\prime KL} w^{0,L} \right) + N_\alpha^K g^0 \right] \\
&- \overline{\nabla}_x^S \cdot \rho_0^{-1} (\mathbb{C}^K \overline{\nabla}_x^S \boldsymbol{u}^{0,K}) - \mathrm{i}\omega \overline{\nabla}_x^S \cdot (\boldsymbol{Q}^K p^0) - \mathrm{i}\omega \boldsymbol{Z}^K \overline{\nabla}_x p^0 = 0 \;,
\end{aligned}
\tag{31}
$$

$$
\begin{aligned}
-\omega^2 &\left[\frac{\overline{\rho_S}^K}{\rho_0} \bar{h}_K w^{0,K} + \sum_{L=I,II} \left(M_{3\alpha}^{KL} u_\beta^{0,L} + M_{33}^{\prime KL} w^{0,L} \right) + N^K g^0 \right] \\
&- \rho_0^{-1} \overline{\nabla}_x \cdot (\boldsymbol{G}^K \overline{\nabla}_x w^{0,K}) - \mathrm{i}\omega \boldsymbol{D}^K \cdot \overline{\nabla}_x p^0 = 0 \;,
\end{aligned}
\tag{32}
$$

$$
\begin{aligned}
-\frac{\omega^2}{c^2} p^0 &+ \overline{\nabla}_x \cdot \boldsymbol{A} \overline{\nabla}_x p^0 - \mathrm{i}\omega \overline{\nabla}_x \cdot (\boldsymbol{B} g^0) - \mathrm{i}\omega \sum_{K=I,II} \overline{\nabla}_x \cdot \left(\boldsymbol{R}^K \boldsymbol{u}^{0,K} + \boldsymbol{P}^K w^{0,K} \right) \\
&+ \sum_{K=I,II} \left(\omega^2 \rho_0 T^K p^0 - \mathrm{i}\omega \boldsymbol{S}^K : \overline{\nabla}_x^S \boldsymbol{u}^{0,K} \right) = -\left(\oint_{I_y^+} g^{1+} - \oint_{I_y^-} g^{1-} \right) \;,
\end{aligned}
\tag{33}
$$

$$
\mathrm{i}\omega \boldsymbol{C} \cdot \overline{\nabla}_x p^0 + \omega^2 F g^0 - \omega^2 \sum_{K=I,II} \left(N^K w^{0,K} + \boldsymbol{N}^K \cdot \boldsymbol{u}^{0,K} \right) = \frac{\mathrm{i}\omega}{\varepsilon_0} [p_{\mathrm{ext}}]_-^+ \;.
\tag{34}
$$

The following symmetries and relationship between the homogenized coefficients can be proved:

$$
\begin{aligned}
&\boldsymbol{X}^K = -\boldsymbol{N}^K \;, \quad W^K = -N^K \;, \quad \boldsymbol{D}^K = \boldsymbol{P}^K \;, \quad \boldsymbol{Z}^K = -(\boldsymbol{R}^K)^T \;, \\
&(\boldsymbol{Q}^K)^T = \boldsymbol{Q}^K = -\boldsymbol{S}^K \;, \quad \boldsymbol{C} = \boldsymbol{B} \;.
\end{aligned}
\tag{35}
$$

After respecting these symmetry relationships in (31)-(34) and denoting

$$\Delta g^1 = \left(\fint_{I_y^+} g^{1+} - \fint_{I_y^-} g^{1-} \right) \;, \tag{36}$$

we can rewrite (31)-(34), as follows:

$$\begin{aligned} -\omega^2 \left[\frac{\overline{\rho_S}^K}{\rho_0} \bar{h}_K \boldsymbol{u}^{0,K} + \sum_{L=I,II} \left(M_{\alpha\beta}^{KL} u_\beta^{0,L} + M_{\alpha 3}^{;KL} w^{0,L} \right) + N_\alpha^K g^0 \right] \\ -\overline{\nabla}_x^S \cdot \rho_0^{-1} (\mathbb{C}^K \overline{\nabla}_x^S \boldsymbol{u}^{0,K}) + \mathrm{i}\omega \overline{\nabla}_x^S \cdot (\boldsymbol{S}^K p^0) + \mathrm{i}\omega \boldsymbol{R}^K \overline{\nabla}_x p^0 = 0 \;, \end{aligned} \tag{37}$$

$$\begin{aligned} -\omega^2 \left[\frac{\overline{\rho_S}^K}{\rho_0} \bar{h}_K w^{0,K} + \sum_{L=I,II} \left(M_{3\alpha}^{KL} u_\beta^{0,L} + M_{33}^{;KL} w^{0,L} \right) + N^K g^0 \right] \\ -\rho_0^{-1} \overline{\nabla}_x \cdot (\boldsymbol{G}^K \overline{\nabla}_x w^{0,K}) - \mathrm{i}\omega \boldsymbol{P}^K \cdot \overline{\nabla}_x p^0 = 0 \;, \end{aligned} \tag{38}$$

$$\begin{aligned} -\frac{\omega^2}{c^2} p^0 + \overline{\nabla}_x \cdot \boldsymbol{A} \overline{\nabla}_x p^0 - \mathrm{i}\omega \overline{\nabla}_x \cdot (\boldsymbol{B} g^0) - \mathrm{i}\omega \sum_{K=I,II} \overline{\nabla}_x \cdot \left(\boldsymbol{R}^K \boldsymbol{u}^{0,K} + \boldsymbol{P}^K w^{0,K} \right) \\ + \sum_{K=I,II} \left(\omega^2 \rho_0 T^K p^0 - \mathrm{i}\omega \boldsymbol{S}^K : \overline{\nabla}_x^S \boldsymbol{u}^{0,K} \right) = -\Delta g^1 \;, \end{aligned} \tag{39}$$

$$\mathrm{i}\omega \boldsymbol{B} \cdot \overline{\nabla}_x p^0 + \omega^2 F g^0 - \omega^2 \sum_{K=I,II} \left(N^K w^{0,K} + \boldsymbol{N}^K \cdot \boldsymbol{u}^{0,K} \right) = \frac{\mathrm{i}\omega}{\varepsilon_0} [p_{\mathrm{ext}}]_-^+ \;. \tag{40}$$

To observe the symmetric structure of the problem, it advantageous to introduce the following matrices:

$$\begin{aligned} \mathbb{M}^{KL} = \begin{bmatrix} M_{\alpha\beta}^{KL} & M_{\alpha 3}^{KL} \\ M_{3\beta}^{LK} & M_{33}^{KL} \end{bmatrix} \;, \quad \mathbb{N} = \begin{bmatrix} N_\alpha^K \\ N^K \end{bmatrix} \;, \quad \mathbb{P} = \begin{bmatrix} S_{\alpha\beta}^K + R_{\alpha\beta}^K \\ P_\beta^K \end{bmatrix} \;. \\ \mathbb{D}^K = \rho_0^{-1} \begin{bmatrix} \mathbb{C}^K & 0 \\ 0 & \boldsymbol{G}^K \end{bmatrix} \;, \qquad \overline{\nabla} \mathbf{u}^K = \begin{bmatrix} \overline{\nabla}^S \boldsymbol{u}^{0,K} \\ \overline{\nabla} w^{0,K} \end{bmatrix} \;, \end{aligned} \tag{41}$$

The mass matrix $\mathbb{M}^{KL}$ is symmetric and represents the “added mass”. The coupling effects are represented by matrices $\mathbb{N}^K$, $\mathbb{P}^K$ and by coefficients $\boldsymbol{B}$. The plate stiffness is represented by $\mathbb{D}^K$ including the bending effects. The anisotropic propagation of the acoustic wave in the fluid is described in terms of the tensor $\boldsymbol{A}$, whereas the transverse impedance of the panel is given by F. The vibroacoustic response is described by the fields $\mathbf{u}^K = (\boldsymbol{u}^{0,K}, w^{0,K})$ satisfying the following differential equations imposed on Γ_0:

$$
\begin{aligned}
-\omega^2\left(m^K \boldsymbol{I} + \sum_{L=I,II} \mathbb{M}^{KL}\right)\mathbf{u}^L - \overline{\nabla}\cdot\mathbb{D}^K\overline{\nabla}\mathbf{u}^K + \mathrm{i}\omega\mathbb{P}^K\overline{\nabla}p^0 - \omega^2\mathbb{N}^K g^0 = \boldsymbol{0}\;, \quad \text{for } K = I, II\;,\\
\mathrm{i}\omega\sum_{L=I,II}\mathbb{P}^L\overline{\nabla}\mathbf{u}^L - \omega^2\frac{1}{c^2}p^0 + \overline{\nabla}\cdot\boldsymbol{A}\overline{\nabla}p^0 - \mathrm{i}\omega\boldsymbol{B}\cdot\overline{\nabla}g^0 = -\Delta g^1\;,\\
-\omega^2\sum_{L=I,II}\mathbb{N}^L\cdot\mathbf{u}^L + \mathrm{i}\omega\boldsymbol{B}\cdot\overline{\nabla}p^0 + \omega^2 F g^0 = \frac{\mathrm{i}\omega}{\varepsilon_0}[p]_-^+\;,\\
\left.\begin{array}{rcl}\bar{\boldsymbol{n}}\cdot\overline{\nabla}p^0 & = & 0\;,\\ \boldsymbol{u}^K & = & 0\;,\; K = I, II\;,\end{array}\right\} \quad \text{on } \partial\Gamma_0\;,
\end{aligned}
\tag{42}
$$

where $[p]_-^+ = p^+ - p^-$ is the jump of the "external field" p across Γ_0 and $m^K = \bar{h}^K\rho_S/\rho_0$.

The Global Acoustic Problem. To conclude this section, we reformulate the global problem imposed in domain Ω^G. The acoustic potential p defined in Ω^G is discontinuous on Γ_0, satisfies the equations (3) with the implicit transmission condition $\mathcal{G}([p]_-^+, g^0) = 0$ is given by (42), where $\boldsymbol{u}^K$ and p^0 serve as the internal variables.

Note that $\overline{\nabla}g^0$ is not needed in the weak formulation of (42). The "unknown" coupling function Δg^1, see (36) can be released to simplify the problem. Another option is to use an iterative algorithm which, in this context, defines Δg^1 using the "old approximation" of the outer acoustic field p. This will be issued in our further papers.

4 Examples

In this section we illustrate the sensitivity of the homogenized coefficients to the geometrical arrangement of the perforated panels. We assume two periodically perforated plates, the first one with the rectangular perforation, the second one with the circular perforation. The local corrector problems are solved using the representative volume elements, one (3D) for the fluid domain Y^* and two (2D) for the compliant plates Ξ_K , see Fig. 2. The geometrical parameters of the perforation (defined with respect to the unit cel Y) are: $a = 1$, $b = 0.6$, $c = 0.3$, $d = 0.5$. The thickness of both the perforated plates is $\bar{h} = 0.08$ and their distance $h_{12} = 0.26$.

We consider the change in the relative "in-plane" position of the holes associated with the two plates, described by the parameter d_c. Fig. 3, illustrates the sensitivity of the homogenized coefficients to the geometrical arrangement.

Figure 4 shows the dependence of the selected homogenized coefficients ($\boldsymbol{B}$, F, $\boldsymbol{P}^1$, $\boldsymbol{P}^2$, $\boldsymbol{R}^1$, $\boldsymbol{R}^2$) on the mutual shift of the perforations (defined by d_c). In particular, $\boldsymbol{B}$, $\boldsymbol{P}^1$, $\boldsymbol{P}^2$ are the most sensitive coefficients responsible for the coupling effects between transverse and surface acoustic waves. These coefficients vanish for $d_c \longrightarrow 0$, so that the 2nd equation in (42) governs the distribution of the acoustic fluid potential p^0 independently of g^0 and plate vibrations $\{\mathbf{u}^K\}$.

5 Conclusion

In this paper the homogenized model of the vibroacoustic interaction on perforated double-plates was presented. The detailed derivation of the model will be considered in a separate paper. Some symmetries of the model due relationship between the homogenized coefficients

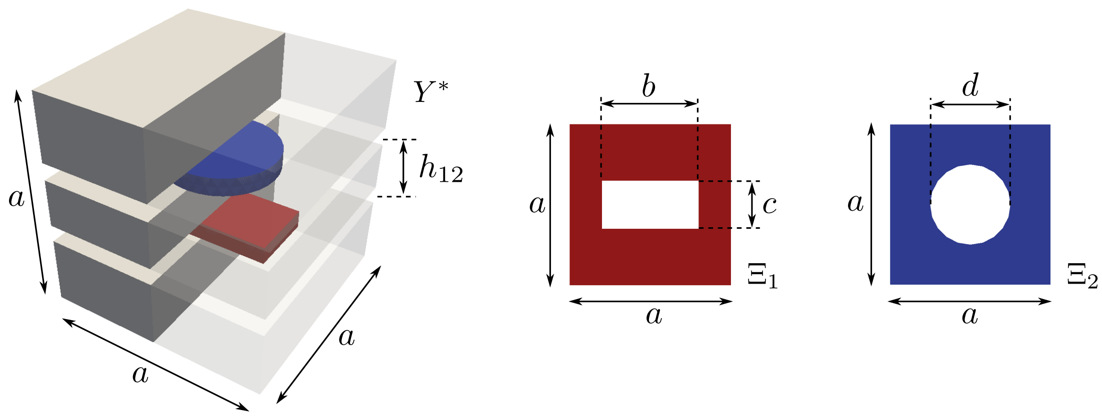

Figure 2: The representative volume elements corresponding to Y^* (3D), Ξ_1 and Ξ_2 (2D) domains.

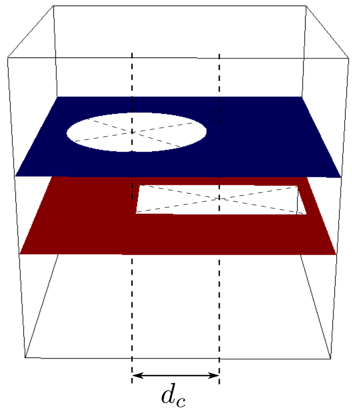

Figure 3: The change in the mutual positions of the holes (perforations) described by the parameter d_c.

were observed. It is worth noting that the plate rotations are not involved explicitly in the homogenized equations, however, the bending stiffness is respected by the homogenized elasticity coefficients. The obtained model represents implicit transmission conditions. As the main advantage, this model enables to reduce quite significantly the computational complexity of solving the acoustic wave propagation in the neighbourhood of the plate panel. Although the model was derived rigorously using the homogenization method, its verification and study of the modelling approximation properties is the further step to be done.

Acknowledgments The research of was supported by the European Regional Development Fund (ERDF), project "NTIS – New Technologies for Information Society", European Centre of Excellence, CZ.1.05/1.1.00/02.0090, in part by the Czech Scientific Foundation projects GACR P101/12/2315.

REFERENCES

[1] R. Cimrman, SfePy - Write Your Own FE Application, in: Proceedings of the 6th European Conference on Python in Science (EuroSciPy 2013), 2014, pp. 65–70, http://arxiv.org/abs/1404.6391.

[2] D. Cioranescu, A. Damlamian, G. Griso, The periodic unfolding method in homogenization, SIAM Journal on Mathematical Analysis 40 (4) (2008) 1585–1620.

[3] A. Cioranescu, D. Damlamian, G. Griso, D. Onofrei, The periodic unfolding method for perforated domains and Neumann sieve models, Journal de Mathématiques Pures et Appliquées 89 (3) (2008) 248–277.

[4] A. Bonnet-Bendhia, D. Drissi, N. Gmati, Mathematical analysis of the acoustic diffraction by a muffler containing perforated ducts, Math. Models and Methods in Appl. Sci. 15 (7) (2005) 1059–1090.

[5] S. e. Jung, Sound absorption of micro-perforated panel, Journal of the Korean Physical Society 50 (2007) 1044–1051.

[6] E. Rohan, V. Lukeš, Homogenization of the acoustic transmission through perforated layer, J. of Comput. and Appl. Math. 234 (2010) 1876–1885.

[7] E. Rohan, B. Miara, Band gaps and vibration of strongly heterogeneous Reissner-Mindlin elastic plates, Comptes Rendus Mathematique 349 (2011) 777–781.

[8] E. Rohan, V. Lukeš, Homogenized perforated interface in acoustic wave propagation – modeling and optimization, in: J. e. Náprstek (Ed.), Proc. of the 10th International Conference on Vibration Problems, ICOVP 2011, Vol. 139 of Springer Proceedings in Physics, Springer, 2011, pp. 321–327.

[9] E. Rohan, V. Lukeš, Sensitivity analysis for optimal design of perforated plates in vobroacoustics: homogenization approach, in: Proceedings of ISMA 2012 – USD 2012, KU Leuven, 2012, pp. 4201–4214.

[10] E. Rohan, V. Lukeš, Homogenized perforated interface in acoustic wave propagation – modeling and optimization, in: Z. D. et.al. (Ed.), Proc. of the 11th International Conference on Vibration Problems, ICOVP 2013, Lisbon, Portugal, 2013, pp. 1–10, (paper 501). http://www.icovp.com.

[11] K. Sakagami, K. Matsutani, M. Morimoto, Sound absorption of a double-leaf microperforated panel with an air-back cavity and a rigid-back wall: Detailed analysis with a Helmholtz-Kirchhoff integral formulation, Applied Acoustics 71 (2010) 411–417.

[12] E. Sanchez-Palencia, Non-homogeneous media and vibration theory, no. 127 in Lecture Notes in Physics, Springer, Berlin, 1980.

[13] F.-A. Stremtan, I. Lupea, Assessing the sound absorption of micro-perforated panels by using the transfer function and the impedance tube, RJAV IX (2) (2012) 94–99, ISSN 1584-7284.

[14] J. Zhou, A. Bhaskar, X. Zhang, Sound transmission through a double-panel construction lined with poroelastic material in the presence of mean flow, Journal of Sound and Vibration 332 (2013) 3724–3734.

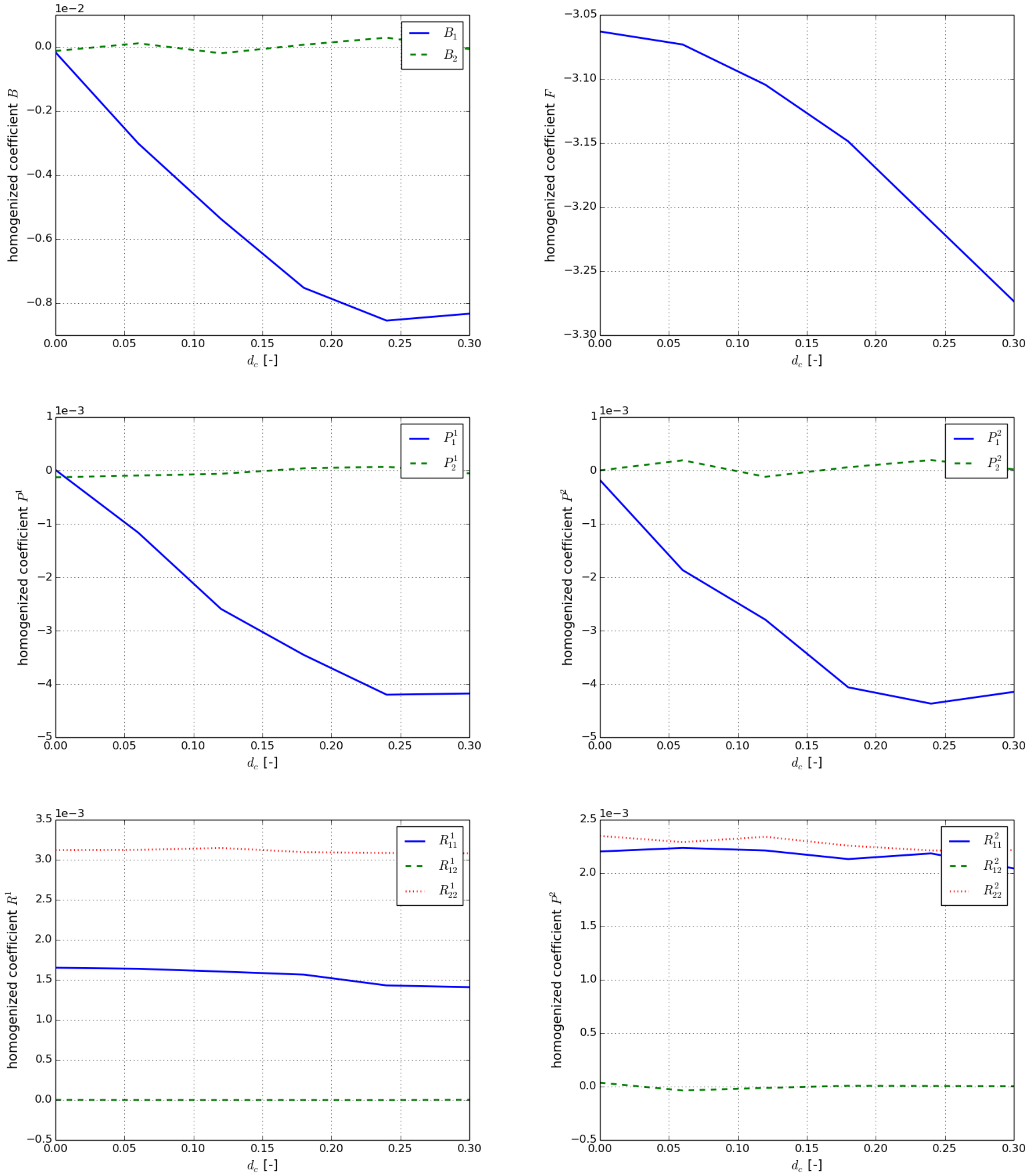

Figure 4: The sensitivity of the homogenized coefficients $\boldsymbol{B}$, F, $\boldsymbol{P}^1$, $\boldsymbol{P}^2$, $\boldsymbol{R}^1$, $\boldsymbol{R}^2$ to the geometrical parameter d_c.